How to cite: *Angew. Chem. Int. Ed.* **2022**, *61*, e202113163
International Edition: doi.org/10.1002/anie.202113163
German Edition: doi.org/10.1002/ange.202113163

VIP **Fluorescent Probes** **Very Important Paper**

# Photocleavable Fluorescent Membrane Tension Probes: Fast Release with Spatiotemporal Control in Inner Leaflets of Plasma Membrane, Nuclear Envelope, and Secretory Pathway

*Javier López-Andarias, Krikor Eblighatian, Quentin T. L. Pasquer, Lea Assies, Naomi Sakai, Sascha Hoogendoorn, and Stefan Matile**

***Abstract:*** *Mechanosensitive flipper probes are attracting interest as fluorescent reporters of membrane order and tension in biological systems. We introduce PhotoFlippers, which contain a photocleavable linker and an ultralong tether between mechanophore and various targeting motifs. Upon irradiation, the original probe is released and labels the most ordered membrane that is accessible by intermembrane transfer. Spatiotemporal control from photocleavable flippers is essential to access open, dynamic or elusive membrane motifs without chemical or physical interference. For instance, fast release with light is shown to place the original small-molecule probes into the innermost leaflet of the nuclear envelope to image changes in membrane tension, at specific points in time of membrane trafficking along the secretory pathway, or in the inner leaflet of the plasma membrane to explore membrane asymmetry. These results identify PhotoFlippers as useful chemistry tools to enable research in biology.*

The imaging of order and particularly physical tension in biomembranes with fluorescent probes is a topic of current concern.[1–3] Beginning with the original **1**, "Flipper" probes have been introduced to tackle this challenge with a planarizable push-pull mechanophore that responds to membrane compression with a red shift in excitation and an increase in fluorescence lifetime (Figure 1, Figure 2 A).[4,5] This mechanism of action differs from alternative approaches that report changes in hydration and viscosity,[6–11] and has been validated in many practical applications.[5] In fluorescence lifetime imaging microscopy (FLIM), flipper probes report high order of membranes at rest with long fluorescence lifetimes, and the increasing tension applied to cellular membranes composed of mixed lipids with increasing lifetime.[12]

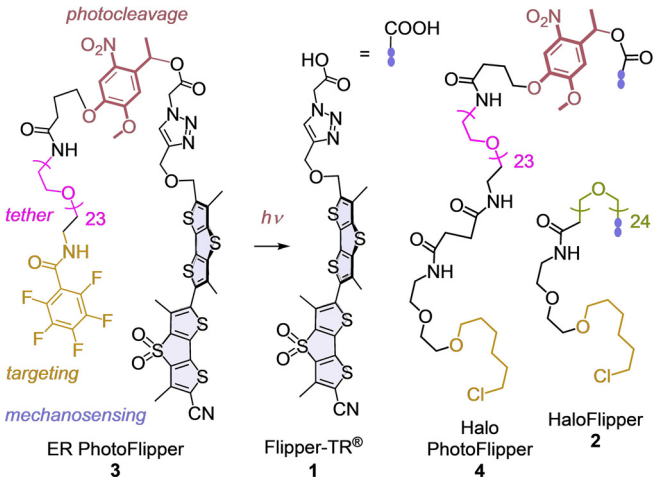


***Figure 1.*** Structure of photocleavable flippers **3** and **4** compared to the original **1** and **2**.

The targeting of fluorescent probes to different organelles inside cells has been widely explored. Probes equipped with empirical "tracker" groups can be simply added to cells and find their targets by different, sometimes unknown mechanisms.[13,14] With the alternative genetic engineering approach, probes are attached to ligands for proteins that are expressed at specific sites.[15] With fluorescent flippers, both strategies have been explored, including HaloFlippers **2** to covalently bind to HaloTags[16] and SupraFlippers to non-covalently bind to streptavidin expressed at the site of interest.[17] This non-covalent targeting allows the release of SupraFlippers in response to chemical stimulation. However, for fast release with spatiotemporal control and minimal chemical interference, photouncaging is the method of choice.[18–25] The possibility to photorelease unmodified probes at specific sites is particularly valuable because the attachment of targeting groups often disturbs the properties of the original probes.[18,19] Here, we introduce PhotoFlippers for the rapid release of the fully optimized and characterized original Flipper-TR **1** to the membrane of interest (MOI) upon irradiation with light.

In PhotoFlippers **3** and **4**, an *o*-nitrobenzyl group[20,23] was selected to minimize overlap with the red-shifted absorption of the flipper probe. This classical photocleavable group and a long tether are inserted between the original Flipper-TR scaffold and targeting motifs that operate by empirical

[*] Dr. J. López-Andarias, K. Eblighatian, Q. T. L. Pasquer, L. Assies, Dr. N. Sakai, Prof. S. Hoogendoorn, Prof. S. Matile
Department of Organic Chemistry, National Centre of Competence in Research (NCCR) Chemical Biology, University of Geneva
Geneva (Switzerland)
E-mail: stefan.matile@unige.ch
Homepage: https://www.unige.ch/sciences/chiorg/matile/

Supporting information and the ORCID identification number(s) for the author(s) of this article can be found under: https://doi.org/10.1002/anie.202113163.

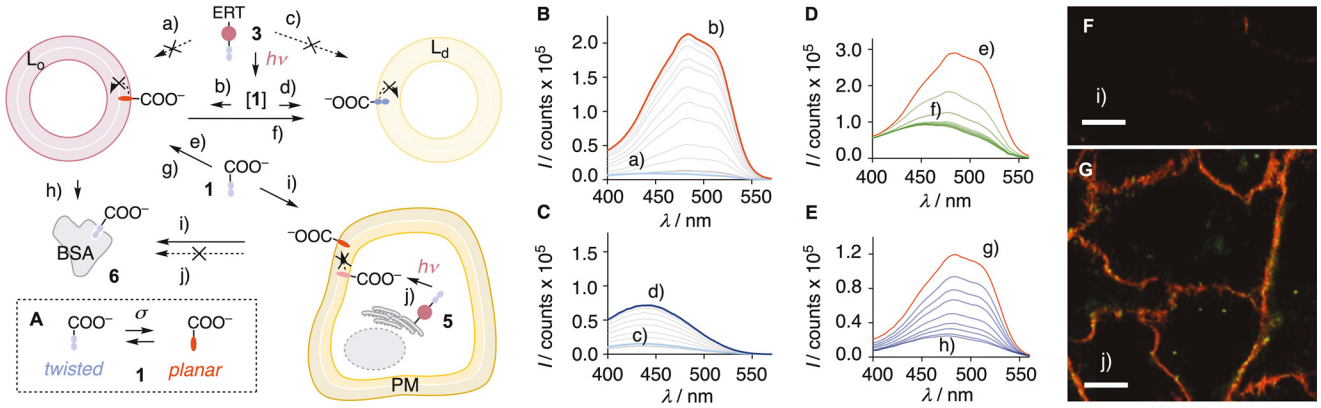


***Figure 2.*** A) Mode of action of **1**, $\sigma$ = compressive force. B) Excitation spectra of **3** (100 nM, $\lambda_{em}$ = 600 nm) in SM/CL LUVs (75 μM) at 25 °C before (a, light blue) and after up to 20 min of bulk irradiation at $\lambda$ = 365 nm (b, grey to red). C) Same as (B) in DOPC LUVs (75 μM) with final spectrum in dark blue (c–d). D) Excitation spectra of **1** (100 nM, $\lambda_{em}$ = 600 nm) in SM/CL LUVs (75 μM) 0 min (e, red), 0.5 to 5 min (f, green) after addition of DOPC LUVs (75 μM). E) Excitation spectra of **1** (40 nM, $\lambda_{em}$ = 600 nm) in SM/CL LUVs after addition of 0 (g, red), 0.25 to 20 μM (h, blue) BSA. F) FLIM image of **1** (1 μM, 15 min) in HK cells after washing with BSA (serum 10%, 3×1 mL, i) and G) of **3** (5 μM, 15 min) after irradiation ($\lambda$ = 365 nm, 3 min) and washing with BSA (serum 10%, 3×1 mL, j). Scale bar: 10 μm.

tracking and genetic engineering, respectively. Both PhotoFlippers were synthesized by adapting established procedures (Scheme S1). Added to large unilamellar vesicles (LUVs) composed of sphingomyelin (SM) and cholesterol (CL), they exhibited weak blue shifted excitation maxima (Figure 2Ba). This poor performance confirmed that the extra-long hydrophilic tether[16] effectively hinders partitioning into liquid-ordered ($L_o$) membranes. Irradiation at 365 nm afforded within $t_{1/2} \approx 3$ min the red-shifted, intense maximum known[5] for **1** in $L_o$ LUVs (Figures 2Bb, S1). Irradiation in the presence of liquid-disordered ($L_d$) dioleoyl phosphocholine (DOPC) LUVs yielded the corresponding bathochromic and weaker maximum (Figure 2C). The conversion of **3** and **4** into **1** upon irradiation in the presence of LUVs was confirmed by HPLC to occur quantitatively within a few minutes (Figure S2).

The pentafluorophenyl group in PhotoFlipper **3** is routinely used to label the endoplasmic reticulum (ER), presumably by nucleophilic aromatic substitution with thiols of proteins at the outer membrane surface.[18,26] Added to HeLa Kyoto (HK) cells, probe **3** labeled the ER with a Pearson correlation coefficient (PCC) = 0.86 for co-localization with ER-Tracker Blue-White DPX (Figures 3A, S3). Irradiation times were finetuned to observe maximal release at minimal phototoxicity, here 2.5 minutes. Eventual non-released probes were considered unproblematic because their fluorescence is much weaker (Figure 2B,C). Irradiation of the resulting conjugate **5** caused an instantaneous and complete migration of flipper fluorescence to the plasma membrane (PM, Figure 3B). This change was much too fast for flipper translocation along the secretory pathway.[17] It thus indicated that, as soon as photoreleased from the ER surface within a few minutes (Figures 2B,C, S2), flipper **1** re-distributes among all membrane leaflets accessible by free diffusion (Figures 2D, S4). Only the most ordered membrane, here the PM, is labeled because planarization of flipper **1** in such membranes suppresses competing non-radiative decay and thus increases emission intensity decisively,[5] as previously illustrated in FLIM images and computational simulations of phase-separated membranes[12,27,28] (Figure 2B,C).

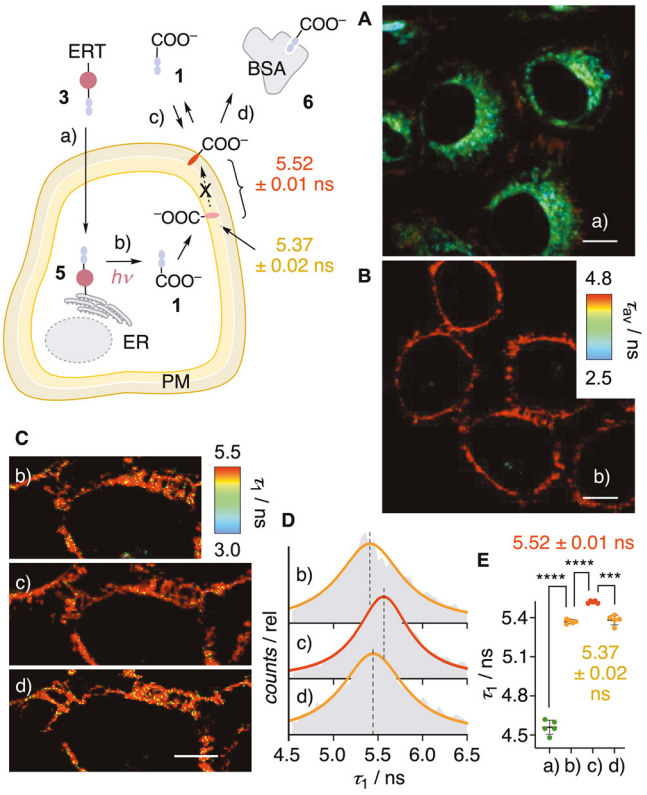


***Figure 3.*** FLIM images of HK cells after A) addition of ER PhotoFlipper **3** (a, 2.5 μM, 15 min), B),Cb) irradiation (b, $\lambda$ = 365 nm, 2.5 min), Cc) subsequent addition of **1** (c, 1 μM, 2 min), and Cd) treatment with media containing BSA (d, serum 10%). Scale bar: 10 μm. D) FLIM histogram associated with the $\tau_1$ component of **1** in stages b–d in (C). E) Fluorescence lifetimes of flipper probes in the four different stages a–d in (A)–(C); statistical significance was determined using Student's *t*-test, ns: $p > 0.05$, *: $p < 0.05$, **: $p < 0.005$, ***: $p < 0.0005$, ****: $p < 0.0001$ (unpaired from a to b, paired from b to c and c to d).

The photo-released **1** thus provides access to the hard to obtain mechanical properties of the PM inner leaflet.[29–33] Biexponential reconvolution of FLIM images gave a $\tau_1 =$ 5.37 ns, which increased to $\tau_1 = 5.52$ ns upon external addition of flipper **1** and returned to the original value upon addition of bovine serum albumin (BSA) to the cell culture medium to remove **1** from the outer leaflet. Although naturally small, the difference in $\tau_1$ is reliable thanks to the direct comparison, and confirmed the lower order of the inner compared to the outer leaflet of the PM. These conclusions were in agreement with recent results from microinjection of probes into different cells,[29] and controls in LUVs and cells. For instance, addition of $L_d$ to $L_o$ LUVs with externally added **1** caused a decrease in intensity and a blue shift of the excitation band with $t_{1/2} \approx 30$ s, confirming instantaneous intermembrane transfer (Figures 2D, S4). Addition of BSA to the same $L_o$ LUVs caused an even stronger loss in intensity, confirming the binding of **1** to BSA ($K_D = 0.7$ μM, Figure S5) and the negligible fluorescence of their complex **6** (Figure 2E). In HK cells, externally added **1** was removed almost completely by washing with BSA-containing media (Figures 2F, S6). The fluorescence of **1** photo-generated from **3** on the ER surface was not affected by the same procedure (Figure 2G). This contrast demonstrated that photo-released **1** stays in the inner leaflet of the PM without flip-flop to the outer leaflet.

Targeting with the complementary, more general, genetically engineered HaloTag was envisioned with photocleavable HaloFlipper **4**.[11,16] Cellular uptake was as efficient as for the uncleavable HaloFlipper **2** ($CP_{50} = 16 \pm 2$ nM, Figure S7).[16,34] PhotoFlipper **4** was applied first to HK cells that transiently express a HaloTag in the luminal side of the Golgi apparatus (GA). Before irradiation, FLIM images showed labeled GA around the nucleus emitting with short lifetime ($\tau_1 = 3.85$ ns, Figure 4A,C, a). After irradiation, the number of labelled subcellular structures increased throughout the cells, and the overall lifetime jumped to $\tau_1 = 4.9$ ns (Figure 4A,C, b). The same experiment repeated with the uncleavable HaloFlipper **2** gave labelled GA emitting with longer and unchanged fluorescence lifetime before and after irradiation ($\tau_1 = 4.37$ ns, Figure 4B,D). These results suggested that both flippers covalently label the same HaloTag inside the GA. While the tethered HaloFlipper in conjugate **7** partitions into the surrounding membrane and reports on order, the slightly longer tether of PhotoFlipper in conjugate **8** prevents partitioning before irradiation, according to the much shorter lifetime observed. Upon irradiation, flipper **1** is released into the inner leaflet of the GA membrane. Unable to flip out, **1** presumably migrates along the secretory pathway from the GA to slowly fuse into the PM. Photoinduced release of **1** from **4** at the luminal side of the ER gave similar results (Figure S8). To elaborate on the mechanics of membrane trafficking along the secretory pathway, such fast release without chemical interference is important to label specific points in time with a narrow distribution; slow release smears labels over several connected sites.[17]

Labeling of the innermost leaflet of the nuclear membrane with tension probes is interesting because it plays a key role in chromatin organization but demanding because fast staining with spatiotemporal control is required to prevent

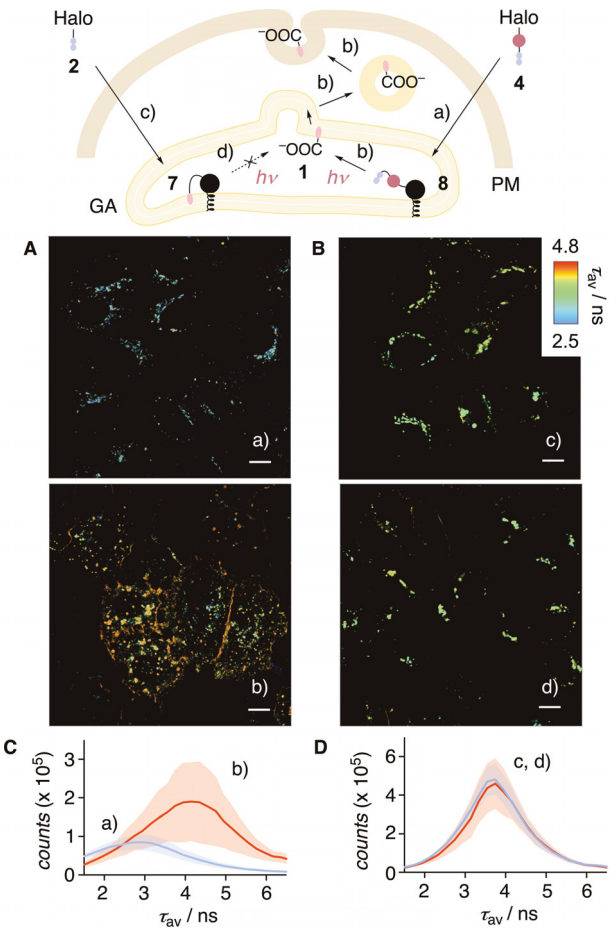


***Figure 4.*** A) FLIM images of HK cells transiently expressing HaloTag in the luminal side of GA labelled with **4** (100 nM, 1 h) before (a) and after (b) bulk irradiation ($\lambda = 365$ nm, 2.5 min). B) Same as (A) with **2** (100 nM, 1 h) before (c) and after (d) irradiation. Scale bars: 10 μm. C) FLIM histograms for **4** in HK cells (A) before (blue, a) and after (red, b) irradiation. D) FLIM histograms for **2** in HK cells (B) before (blue, c) and after (red, d) irradiation. Black filled circles represent HaloTags.

diffusion to the outermost leaflet and the cytosol (Figure 5).[35,36] Thus, HaloTags equipped with nuclear localization sequence (NLS) were stably expressed in HK cells (Figure S9a,b). Addition of **4** followed by an incubation with BSA resulted in labeling of the nuclear envelope, as well as the nucleus (Figures 5Aa, S9c–f). Before irradiation, the fluorescence lifetime $\tau_1$ was very short, even after selecting only the nuclear envelope (3.92 ns), supporting LUV results that caged flippers like **9** partition poorly into membranes.

Photocleavage caused an increase in fluorescence lifetime to $\tau_1 = 4.3$ ns in the nuclear envelope (Figure 5Ab) and a decrease in fluorescence intensity inside the nucleus (clearly visible in Figure 5D). The same lifetime change occurred upon focused irradiation on one nucleus using a FRAP module, demonstrating the spatial controllability of the process (Figure 5D). This change was consistent with the photocleavage of low-emitting conjugates **9** to release **1** into the inner leaflet of the nuclear envelope. With time, **1** migrated from the nuclear envelope to the PM, which is feasible through the nuclear pore[36] (Figure 5Ac). Hyper-

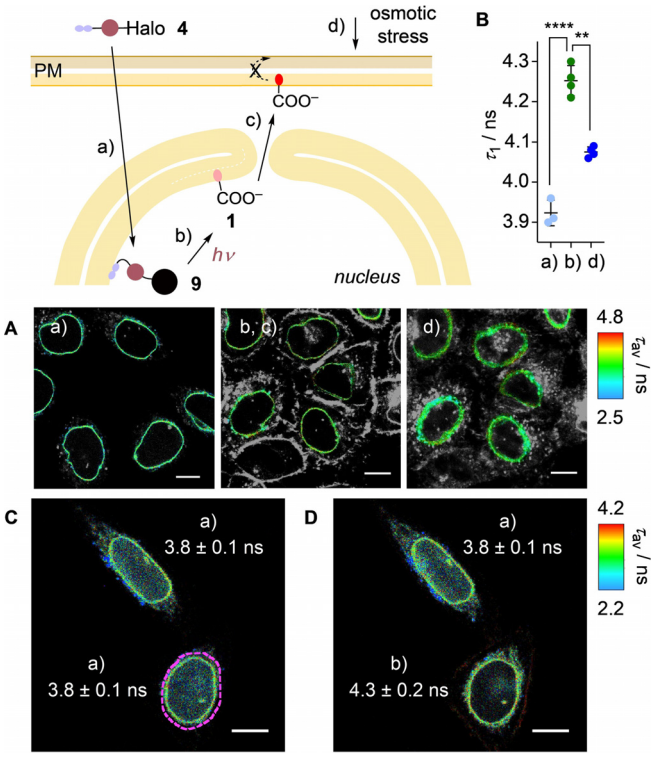


***Figure 5.*** A) Masked FLIM images of HK cells stably expressing HaloTag-NLS labelled with **4** (250 nM, 1 h) a) before and b, c) after bulk irradiation and d) after addition of sucrose (0.5 M). Only the nuclear envelope is highlighted (original images: Figure S10). B) Fluorescence lifetimes of **4** in stages a, b, d in A; statistical significance was determined using Student's t-test, as in Figure 3 (unpaired from a to b, paired from b to c). C) Same as A without any mask of the nuclear envelope, a, with dashed purple line marking the area to be irradiated. D) Same as (C), after irradiation ($\lambda = 405$ nm FRAP module, 5 µW, 30 s) in marked area, with fluorescence lifetime for each cell (values in (C), (D) represent $\tau_1 \pm$ SD, using the nuclear envelope as mask). Scale bars: 10 µm.

osmotic stress caused significant shape changes outside the nuclear membrane (Figure 5 Ad). Thus, focused analysis was performed of the nuclear envelope to give a lifetime decrease from $\tau_1 = 4.25$ ns to $\tau_1 = 4.08$ ns (Figure 5 Ab–d). The extent of lifetime change was in the range observed previously in other organelles, suggesting that hyperosmotic stress also reduces the membrane tension in the innermost leaflet of the nuclear envelope.

Taken together, this study introduces photocleavable flipper probes **3** and **4**, which release small molecule mechanophores to image order and tension of any membrane of interest within cells. Facile and fast photoinduced release provides access to spatiotemporal control without chemical interference. The released probe is identical with the original, optimized Flipper-TR **1**. This is important because it removes all possible effects of targeting groups on function. The released Flipper-TR **1** labels the leaflet of highest order that is accessible without flip-flop. The importance of rapid labeling with spatiotemporal control is exemplified with the innermost leaflet of the nuclear envelope and inner leaflets along the secretory pathway. Both sites of interest are elusive otherwise because of their dynamic nature, the former being connected to the outermost leaflet, and the latter in transit between ER, GA and PM. The importance of labeling with leaflet-level precision is further exemplified with the inner leaflet of the PM, which is confirmed to be less ordered than the outer leaflet. These examples on use in biology demonstrate that the next level of precision reached in imaging membrane order and tension is significant. They identify PhotoFlippers as the chemistry tools needed to address current challenges in biology that are otherwise intractable, and open attractive perspectives for future development.[37]

## Acknowledgements

We thank R. Lim (Biozentrum Basel) for discussions, J. A. Kritzer (Tufts University) and D. Toomre (Yale University) for providing materials, N. Winssinger for the access to LED setup, A. Roux for FLIM, the NMR, the MS, and the Bioimaging and ACCESS platforms for services, and University of Geneva, the Swiss National Centre of Competence in Research (NCCR) Molecular Systems Engineering, the NCCR Chemical Biology, and the Swiss NSF for financial support (S.H., 189246; S.M., 175486, 204175). K.E. acknowledges a Werner Fellowship. Open access funding provided by Université de Genène.

## Conflict of Interest

The University of Geneva has licensed four Flipper-TR probes including **1** to Spirochrome for commercialization.

**Keywords:** fluorescent probes · mechanosensitivity · membrane asymmetry · membrane tension · photocleavage

[1] B. Pontes, P. Monzo, N. C. Gauthier, *Semin. Cell Dev. Biol.* **2017**, *71*, 30–41.
[2] E. Sitarska, A. Diz-Muñoz, *Curr. Opin. Cell Biol.* **2020**, *66*, 11–18.
[3] A. Saric, S. A. Freeman, *Front. Cell Dev. Biol.* **2021**, *8*, 611326.
[4] A. Fin, A. Vargas Jentzsch, N. Sakai, S. Matile, *Angew. Chem. Int. Ed.* **2012**, *51*, 12736–12739; *Angew. Chem.* **2012**, *124*, 12908–12911.
[5] T. Kato, K. Strakova, J. García-Calvo, N. Sakai, S. Matile, *Bull. Chem. Soc. Jpn.* **2020**, *93*, 1401–1411.
[6] A. S. Klymchenko, *Acc. Chem. Res.* **2017**, *50*, 366–375.
[7] D. I. Danylchuk, P.-H. Jouard, A. S. Klymchenko, *J. Am. Chem. Soc.* **2021**, *143*, 912–924.
[8] C.-H. Wu, Y. Chen, K. A. Pyrshev, Y.-T. Chen, Z. Zhang, K.-H. Chang, S. O. Yesylevskyy, A. P. Demchenko, P.-T. Chou, *ACS Chem. Biol.* **2020**, *15*, 1862–1873.
[9] M. Páez-Pérez, I. López-Duarte, A. Vyšniauskas, N. J. Brooks, M. K. Kuimova, *Chem. Sci.* **2021**, *12*, 2604–2613.
[10] Y. Zheng, Y. Ding, J. Ren, Y. Xiang, Z. Shuai, A. Tong, *Anal. Chem.* **2020**, *92*, 14494–14500.
[11] J. E. Chambers, M. Kubánková, R. G. Huber, I. López-Duarte, E. Avezov, P. J. Bond, S. J. Marciniak, M. K. Kuimova, *ACS Nano* **2018**, *12*, 4398–4407.
[12] A. Colom, E. Derivery, S. Soleimanpour, C. Tomba, M. D. Molin, N. Sakai, M. González-Gaitán, S. Matile, A. Roux, *Nat. Chem.* **2018**, *10*, 1118–1125.

[13] N. Trinh, K. A. Jolliffe, E. J. New, *Angew. Chem. Int. Ed.* **2020**, *59*, 20290 – 20301; *Angew. Chem.* **2020**, *132*, 20466 – 20479.
[14] P. Gao, W. Pan, N. Li, B. Tang, *Chem. Sci.* **2019**, *10*, 6035 – 6071.
[15] J. Liu, Z. Cui, *Bioconjugate Chem.* **2020**, *31*, 1587 – 1595.
[16] K. Straková, J. López-Andarias, N. Jiménez-Rojo, J. E. Chambers, S. J. Marciniak, H. Riezman, N. Sakai, S. Matile, *ACS Cent. Sci.* **2020**, *6*, 1376 – 1385.
[17] J. López-Andarias, K. Straková, R. Martinent, N. Jiménez-Rojo, H. Riezman, N. Sakai, S. Matile, *JACS Au* **2021**, *1*, 221 – 232.
[18] N. Wagner, M. Stephan, D. Höglinger, A. Nadler, *Angew. Chem. Int. Ed.* **2018**, *57*, 13339 – 13343; *Angew. Chem.* **2018**, *130*, 13523 – 13527.
[19] S. Farley, A. Laguerre, C. Schultz, *Curr. Opin. Chem. Biol.* **2021**, *65*, 42 – 48.
[20] G. C. R. Ellis-Davies, *Acc. Chem. Res.* **2020**, *53*, 1593 – 1604.
[21] K. Hüll, J. Morstein, D. Trauner, *Chem. Rev.* **2018**, *118*, 10710 – 10747.
[22] L. Josa-Culleré, A. Llebaria, *ChemPhotoChem* **2021**, *5*, 296 – 314.
[23] C. Aonbangkhen, H. Zhang, D. Z. Wu, M. A. Lampson, D. M. Chenoweth, *J. Am. Chem. Soc.* **2018**, *140*, 11926 – 11930.
[24] S. Feng, T. Harayama, S. Montessuit, F. P. David, N. Winssinger, J.-C. Martinou, H. Riezman, *eLife* **2018**, *7*, e34555.
[25] A. Sailer, F. Ermer, Y. Kraus, F. H. Lutter, C. Donau, M. Bremerich, J. Ahlfeld, O. Thorn-Seshold, *ChemBioChem* **2019**, *20*, 1305 – 1314.
[26] A. Goujon, A. Colom, K. Straková, V. Mercier, D. Mahecic, S. Manley, N. Sakai, A. Roux, S. Matile, *J. Am. Chem. Soc.* **2019**, *141*, 3380 – 3384.
[27] K. Strakova, A. I. Poblador-Bahamonde, N. Sakai, S. Matile, *Chem. Eur. J.* **2019**, *25*, 14935 – 14942.
[28] G. Licari, K. Strakova, S. Matile, E. Tajkhorshid, *Chem. Sci.* **2020**, *11*, 5637 – 5649.
[29] J. H. Lorent, K. R. Levental, L. Ganesan, G. Rivera-Longsworth, E. Sezgin, M. Doktorova, E. Lyman, I. Levental, *Nat. Chem. Biol.* **2020**, *16*, 644 – 652.
[30] A. V. Weigel, C.-L. Chang, G. Shtengel, C. S. Xu, D. P. Hoffman, M. Freeman, N. Iyer, J. Aaron, S. Khuon, J. Bogovic, W. Qiu, H. F. Hess, J. Lippincott-Schwartz, *Cell* **2021**, *184*, 2412 – 2429.
[31] A. Gupta, T. Korte, A. Herrmann, T. Wohland, *J. Lipid Res.* **2020**, *61*, 252 – 266.
[32] P. F. Devaux, *Biochemistry* **1991**, *30*, 1163 – 1173.
[33] M. Doktorova, J. L. Symons, I. Levental, *Nat. Chem. Biol.* **2020**, *16*, 1321 – 1330.
[34] L. Peraro, K. L. Deprey, M. K. Moser, Z. Zou, H. L. Ball, B. Levine, J. A. Kritzer, *J. Am. Chem. Soc.* **2018**, *140*, 11360 – 11369.
[35] N. Zuleger, M. I. Robson, E. C. Schirmer, *Nucleus* **2011**, *2*, 339 – 349.
[36] B. W. Hoogenboom, L. E. Hough, E. A. Lemke, R. Y. H. Lim, P. R. Onck, A. Zilman, *Phys. Rep.* **2021**, *921*, 1 – 53.
[37] Original data: https://doi.org/10.5281/zenodo.5585965.

Manuscript received: September 28, 2021
Revised manuscript received: October 25, 2021
Accepted manuscript online: November 4, 2021
Version of record online: November 23, 2021